Structural and electrical properties of antiferroelectric lead zirconate thin films prepared by reactive magnetron co-sputtering

K. YAMAKAWA, K. WA GACHIGI, S. TROLIER-McKINSTRY, J. P. DOUGHERTY
Center for Dielectric Studies, Intercollege Materials Research Laboratory, The Pennsylvania State University, University Park, PA 16802, USA

The structural and electrical properties of antiferroelectric lead zirconate thin films were investigated. The films were prepared by a reactive magnetron co-sputtering method followed by rapid thermal annealing. The crystallized films showed (240) preferred orientation on platinum-coated silicon substrates. The lead content in the films was found to affect the crystallization temperatures, the preferred orientation, the film morphology and the electrical properties. In particular, the hysteresis behaviour is sensitive to the amount of lead. The electric field forced transformation from the antiferroelectric phase to the ferroelectric phase was very similar to that observed in single crystals at room temperature, with a maximum polarization value of 70 $\mu C\,cm^{-2}$. The average field required to excite the ferroelectric state and that for reversion to the antiferroelectric state were 290 $kV\,cm^{-1}$ and 180 $kV\,cm^{-1}$ respectively. The dielectric constant was 200 with an associated loss of 0.05 at 1 MHz. The Curie temperature was 248 °C at 1 kHz. The conduction mechanism of the films was similar to that observed for lead zirconate titanate films.

1. Introduction

Advances in thin film preparation and integration techniques are making ferroelectric and dielectric thin films more attractive for possible applications in microelectronic, micro-optical and microelectromechanical systems (MEMS). The unique properties of ferroelectrics and dielectrics permit the design of new kinds of passive devices, transducers and sensors by using semiconductor technology and integrating them into silicon circuits. Lead-based perovskite ferroelectrics such as lead zirconate titanate and lead titanate, and dielectrics such as barium strontium titanate have been studied extensively in recent years. Good charge storage ability as well as stability during processing and superior electrical characteristics are required in order to use these materials as capacitors on semiconductor devices. The piezoelectric properties and pyroelectric properties of such films are used [1] in integrated transducers such as microactuators and micromotors [2], hybrid sensors such as IR detectors and acceleration sensors, and electro-optical devices such as light switches, frequency modulators and wave guides [3].

Antiferroelectrics are alternatives to ferroelectrics and other dielectrics in these applications. Antiferroelectric (AFE) materials are those in which the ionic chains are polarized spontaneously and the adjacent chains of ions of one kind are polarized in the opposite direction, so that there is no net spontaneous polarization [4]. Lead zirconate ($PbZrO_3$) was the first compound identified as an antiferroelectric [5]. An electric field forced phase transformation from the AFE phase to a ferroelectric (FE) phase occurs in $PbZrO_3$ because of the small free energy difference between the two phases. Fesenko *et al.* [6] have reported on phase transformations which occur in $PbZrO_3$ single crystals. It was observed that different hysteresis loops can be induced at different temperatures and electric fields.

The AFE to FE transformation results in a large strain in the material caused by the difference in volume between the two phases. Several papers have been published on the modification of $PbZrO_3$ to achieve a large transformation strain. It has been suggested that tin doped lead zirconate titanate can demonstrate strains up to around 1% [7–9]. This is extremely interesting for transducer applications. Typical double hysteresis loops resulting from the field forced AFE–FE phase transformation are useful for charge storage devices. The switching releases a large amount of charge when the applied electric field is removed. Conversely, the linear section of the polarization-electric field curve (i.e. the low field AFE region) can be used for capacitor applications. This has the advantage of bias-independent capacitance coupled with a reasonably good volumetric efficiency.

In bulk ceramics, however, the AFE–FE transformation is difficult to observe at room temperature, as the electric field required to induce phase switching is often larger than the dielectric strength. Brodeur *et al.* [9] did, nevertheless, observe multiple phase transitions in AFE bulk ceramics. However, there are several recent reports that show that $PbZrO_3$ thin films will undergo room temperature field-induced phase switching with appreciable induced strains [10–18].

$PbZrO_3$ thin films prepared by reactive magnetron co-sputtering were reported recently, in which the electric field induced transformation was observed for (240) oriented films [19]. In this work, the effect of Pb content on the structural and electrical properties of these films is described in detail. Data on the temperature dependence of the permittivity and conduction is also reported.

2. Experimental procedure

$PbZrO_3$ thin films were prepared by a reactive magnetron sputtering method. Individual three inch diameter targets of Pb and Zr were employed and controlled with independent power supplies. A detailed explanation of the system was given in previous reports [19, 20]. The Pb content in the films was changed by controlling the power to the Pb target. Ar/O_2 in the ratio of 90/10 was used as the background gas with a total gas pressure of 10 m Torr. All films were deposited on unheated Pt(200 nm)/Ti(20 nm)/SiO_2/Si substrates. Following deposition, the films were crystallized using rapid thermal annealing (RTA). The Pt film had a (1 1 1) preferred orientation. In order to achieve high reproducibility of the films, the operating power, voltage and current for each d.c. plasma was monitored during the depositions. The sputtering operation was controlled mainly by current because the operating voltage gradually increased after several runs. This phenomenon was caused by the degradation of the surface of the Pb target. Small cone-shaped bumps were observed on the degraded Pb target. When these values changed, the targets were polished to return them to their initial state. The power for the Zr target was kept at a constant value of 250 W and that for the Pb target was controlled by changing the current value from 40 to 65 mA. The corresponding powers ranged from 12 to 21 W. Since the films shrank significantly during the heat treatment, the room temperature deposition/RTA processing cycle was repeated four times to reach 0.3 μm thick films without serious cracks in the films. The annealing time was 30 s for each layer.

The crystal structure and microstructure of the films were observed by X-ray diffraction (XRD) and scanning electron microscopy (SEM). Film thicknesses were measured by a profilometer. Typical film thicknesses were between 0.3 and 0.35 μm. A d.c. plasma emission spectrometer (DCP) was used to determine the composition. The films were first dissolved in a mixed acid solution ($H_2O:HCl:HNO_3$: $HF = 5:2:2:1$) and the emission spectroscopy was conducted on the resulting solution. Electrical measurements were carried out on films with 0.6 mm diameter gold electrodes. Hysteresis behaviour and capacitance–voltage curves were measured using a Radiant Technologies RT66A tester. An impedance analyser (HP4192A) was used to measure the dielectric constant and its frequency dependence. The measurement of the temperature dependence of dielectric constant was performed by a computer controlled furnace and a LCR meter (HP4274). The $I-V$ related measurements were carried out using a HP4140B pA meter with a built-in d.c. voltage supply.

3. Results and discussion

3.1. Structural properties

Fig. 1 shows XRD patterns for $PbZrO_3$ films annealed at various temperatures. The films were deposited

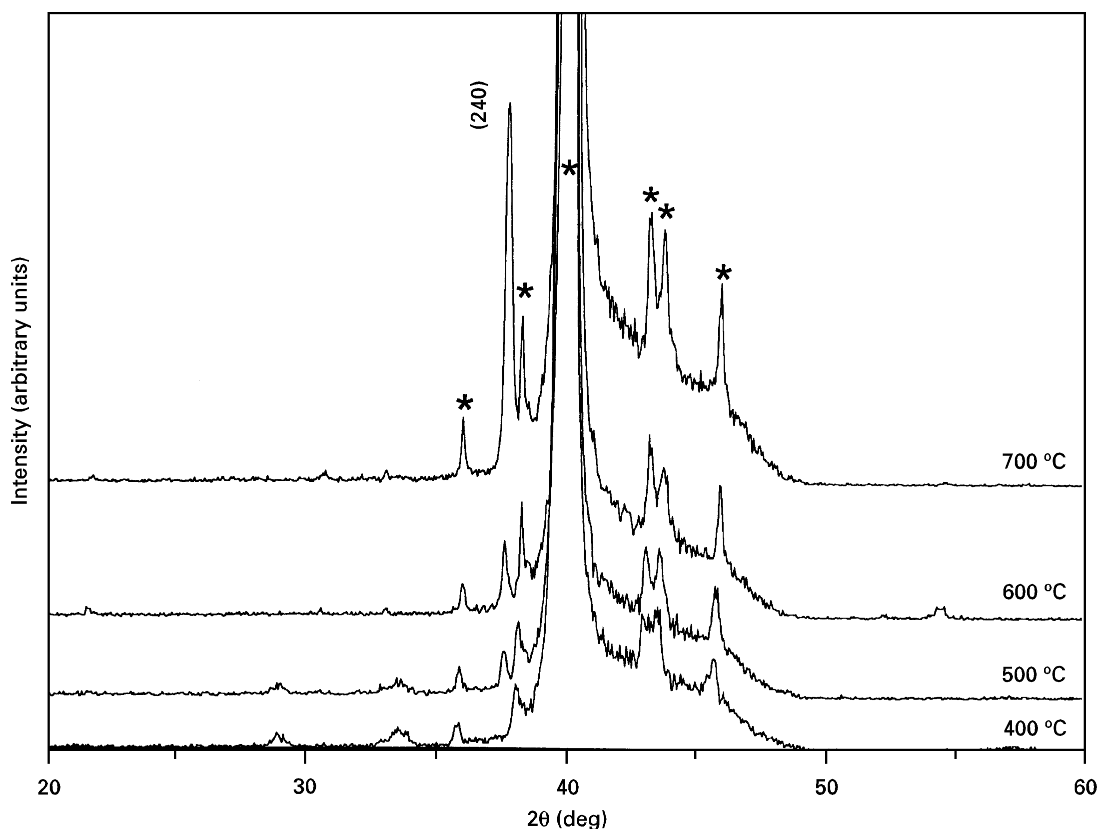

Figure 1 X-ray diffraction patterns for rapid thermal annealed $PbZrO_3$ films at temperatures from 400 to 700 °C. Films were deposited at 56 mA for Pb target. Substrate peaks are indicated by *.

with the current for the Pb target of 56 mA. The Pb/Zr ratio was 1.39 for this film before annealing. It can be observed that the crystallization starts at 500 °C and that the films show (240) preferred orientations when indexed on the orthorhombic unit cell (JCPDS 35-739 or 20-608). 700 °C RTA seems to be sufficient to obtain well crystallized films of $PbZrO_3$. The crystal structure of the (240) plane in orthorhombic $PbZrO_3$ corresponds to that of the (1 1 1) plane in a pseudocubic structure. The oxygen sublattice in this plane

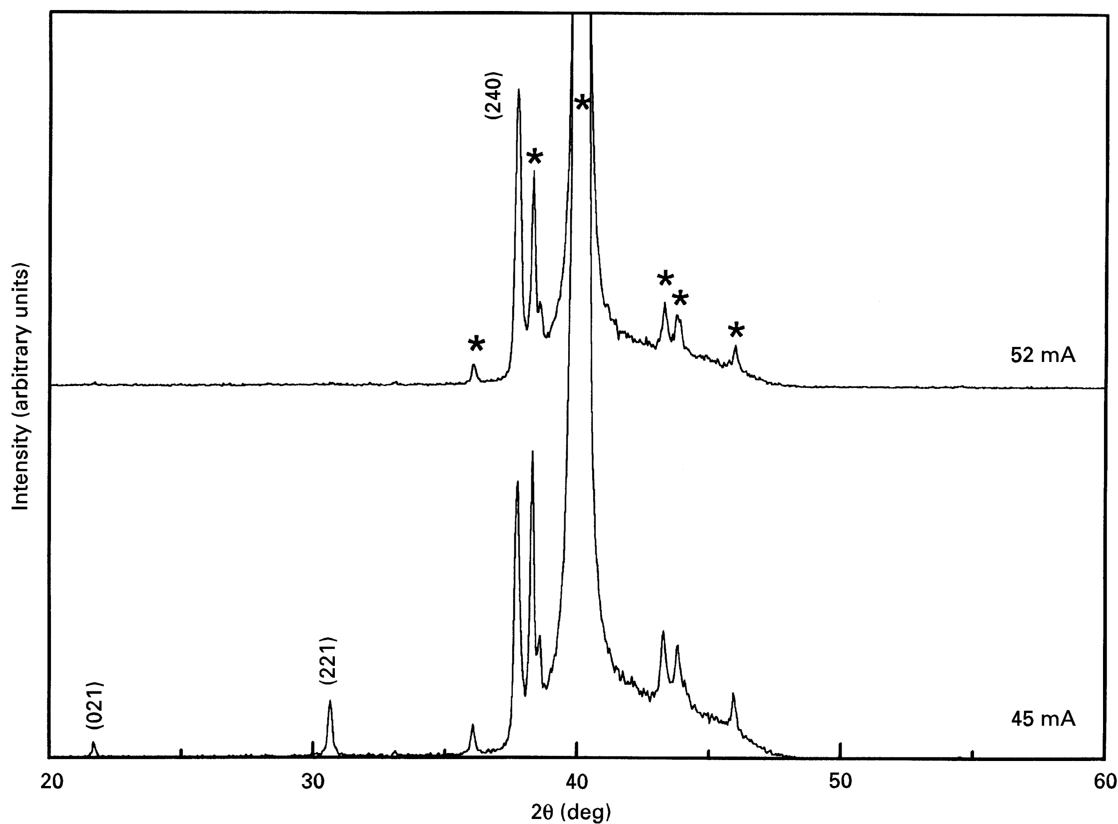

Figure 2 X-ray diffraction patterns indicating different preferred orientations. Currents for Pb target are shown in the figure.

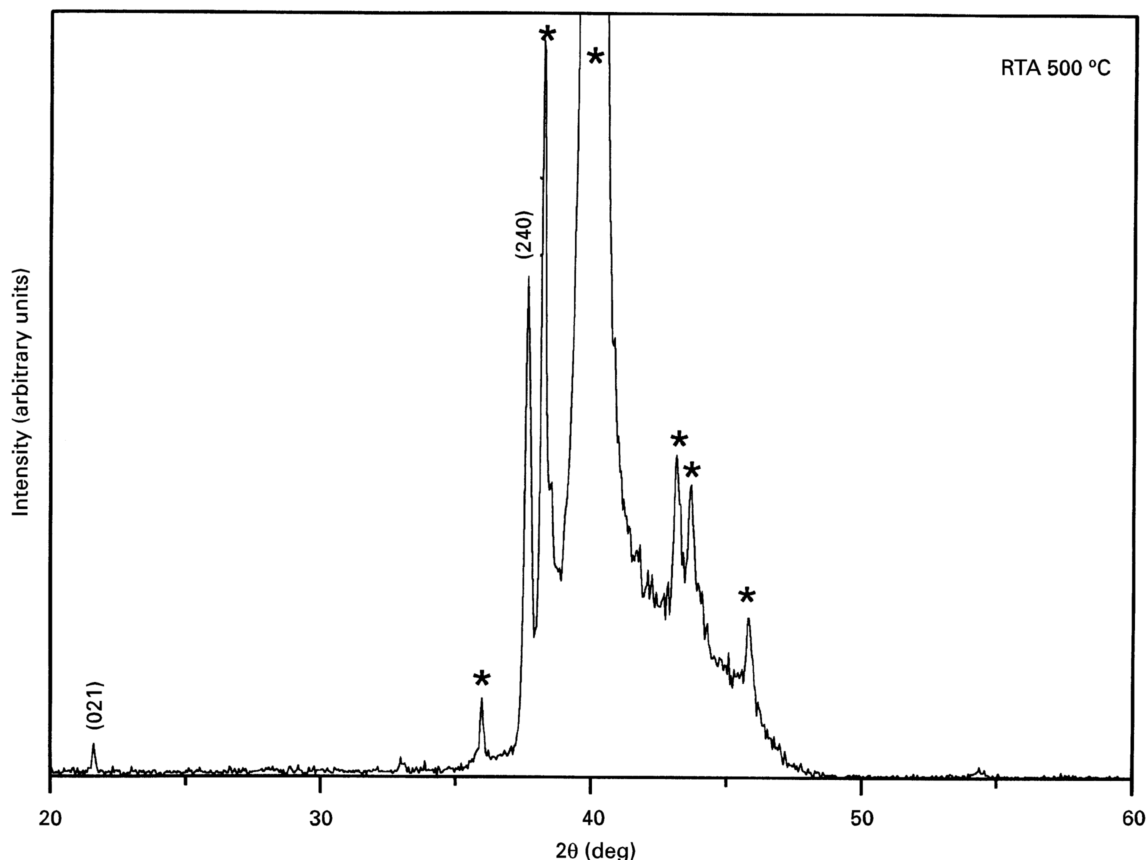

Figure 3 XRD pattern of $PbZrO_3$ film prepared at the lowest temperature. Current for Pb was 52 mA.

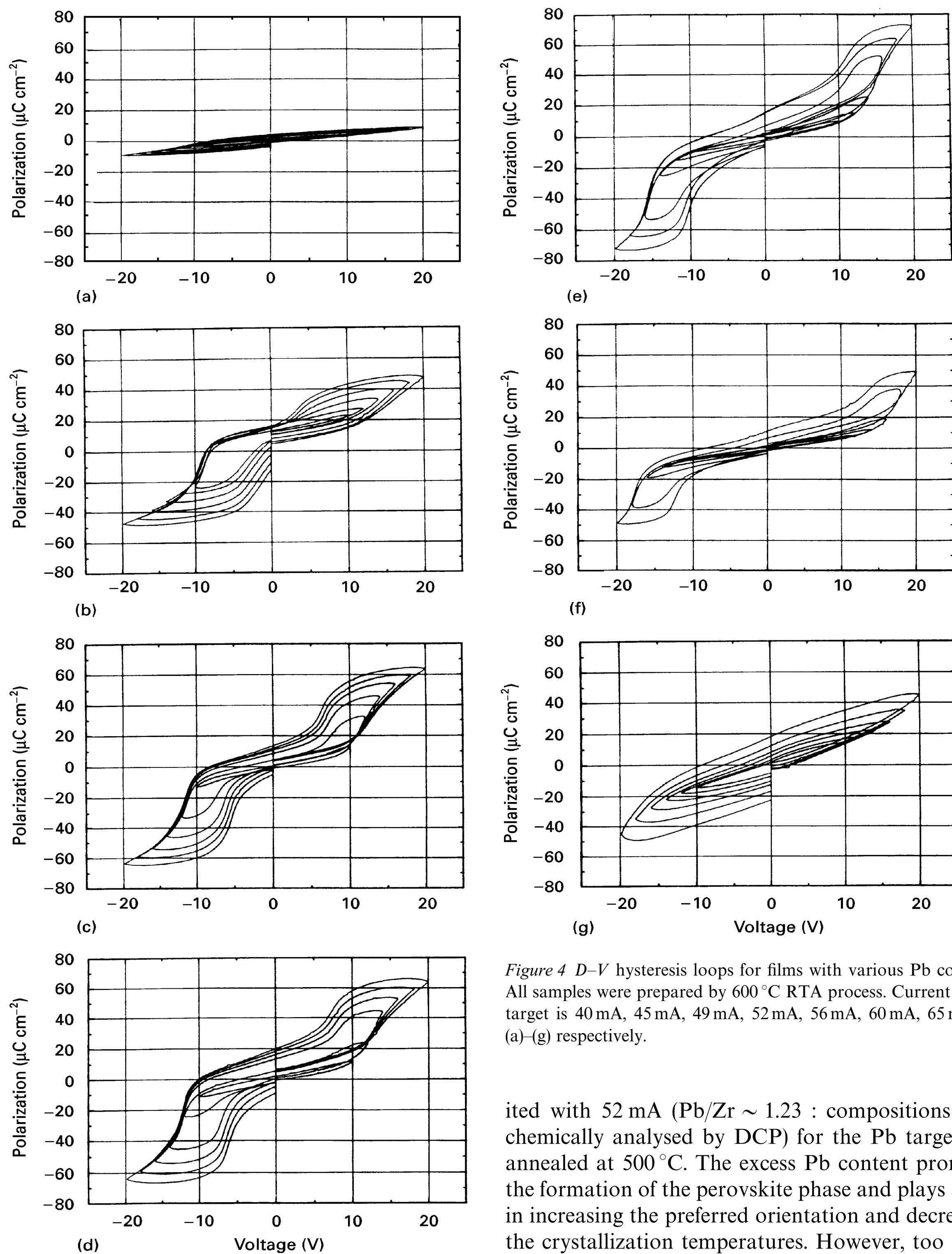

Figure 4 *D–V* hysteresis loops for films with various Pb contents. All samples were prepared by 600 °C RTA process. Current for Pb target is 40 mA, 45 mA, 49 mA, 52 mA, 56 mA, 60 mA, 65 mA for (a)–(g) respectively.

resembles the Pt arrangement in the substrate. The lattice mismatch between the two is around 5 to 6%. Thus, films with (240) preferred orientation are assumed to have compressive stresses in the plane from the lattice-mismatch standpoint. However, tensile stresses also can be expected due to the difference in thermal expansion coefficient, as that of the substrate is dominated by the Si. Effects that seem to come from the stresses will be described later.

It was also seen that a pyrochlore phase formed for RTA treatments below 400 °C. The crystallization of the perovskite phase occurred at 500 °C in Pb excess films. Fig. 2 shows the XRD pattern of the film deposited with 52 mA (Pb/Zr ~ 1.23 : compositions were chemically analysed by DCP) for the Pb target and annealed at 500 °C. The excess Pb content promotes the formation of the perovskite phase and plays a role in increasing the preferred orientation and decreasing the crystallization temperatures. However, too much excess Pb suppressed the formation of both single phase perovskite films and the degree of preferred orientation (see for example, the film deposited at 65 mA to the Pb target). In the case of Pb deficiency, if the Pb/Zr ratio was around 0.8, the perovskite phase was observed by annealing at higher temperatures. A comparison between a $PbZrO_3$ film deposited at 52 mA and one at 45 mA (Pb/Zr ~ 0.83) is displayed in Fig. 3. The former film has (240) preferred orientation while the latter has weaker preferred orientation.

The same tendency was observed for films prepared with too much Pb excess. The mechanisms of preferred orientation in crystal growth have been explained in several papers [13, 21]. There are many parameters that affect preferred orientation of films.

These include; 1) the characteristics of substrates, such as the crystal structures, and their reactivity with deposited films, 2) impurities between the substrates and films, 3) microstructure and composition of films, 4) heat treatment conditions such as heating rate, temperature and time, 5) internal stresses in films, 6) surface energy and interfacial energy of the materials used and 7) structures of film precursors. Non-stoichiometry of Pb changes the microscopic crystallization steps and seems to lead to different crystal structures and crystallization temperatures. It was also found that for similar sputtering and annealing conditions, some films showed more preferred orientation than others. It is believed that this is due to small variations in the Pb content. However, it is also possible that the diffusion of Ti in the bottom electrode may affect the preferred orientation. We obtained randomly oriented $PbZrO_3$ films on $Pt/SiO_2/Si$ substrates without a Ti adhesion layer.

From the SEM observations, the grains were found to have a columnar structure and the average grain size was 0.3–0.5 μm. There were a few cracks observed in the films prepared by the step depositions. This grain size seems to be sufficiently large to permit observation of properties comparable to bulk ceramic $PbZrO_3$.

3.2. Phase transformation

The electric field-induced transformation from the AFE phase to the FE phase was measured for $PbZrO_3$ films with various Pb contents. Fig. 4a to g shows the change of hysteresis loops as a function of Pb content. The measured films were deposited at 40–65 mA (Pb/Zr = 0.83–1.78) for the Pb target and annealed at 600 °C for 30 s. The films deposited at 45–60 mA showed the transformation from the AFE phase to the FE phase. In particular, the films with a Pb/Zr ratio of 1.2 (49–52 mA) have distinct double hysteresis loops. These films seem to have the stoichiometric composition after the evaporation of Pb by annealing. In the case of 600 °C annealed samples, strong peaks of the perovskite phase were observed for these films. The electric fields of the AFE–FE transitions increased with increasing Pb content. It is possible that an amorphous phase of PbO_x which has a low dielectric constant, exists in the grains or at the grain boundaries, and decreases the practical voltages applied to the AFE grains. A decrease in dielectric constant was observed for the films with excess Pb content. The fact that polarization values at which the transformation from the AFE phase to FE phase occurred were constant at about 20 $\mu C\,cm^{-2}$ supports this explanation. For the 65 mA deposition, the film seemed to be lossy and had a rounded hysteresis loop. Low resistivity Pb and PbO_x phases at the grain boundary could be responsible for this. In contrast, the polarization was lower for the Pb-deficient films. This is attributed to a decrease in the amount of the AFE phase present.

The annealing temperature dependence of the D-E curves is shown in Fig. 5. The polarization value increased with increasing RTA temperature. The result is consistent with the crystallinity of the $PbZrO_3$ films. The films annealed at 700 °C have narrow hysteresis loops with a maximum polarization value of 70 $\mu C\,cm^{-2}$. The average field required to induce the FE state from the AFE state and that for the reversion to the AFE phase from the FE phase were found to be 290 $kV\,cm^{-1}$ and 180 $kV\,cm^{-1}$ respectively, by calculation from the applied voltages of the maximum peaks of capacitance. The data is similar to that observed in single crystals [6]. Fig. 6 shows a double hysteresis for a 52 mA deposited film annealed at 500 °C. A polarization value of 60 $\mu C\,cm^{-2}$ was obtained despite the low annealing temperature.

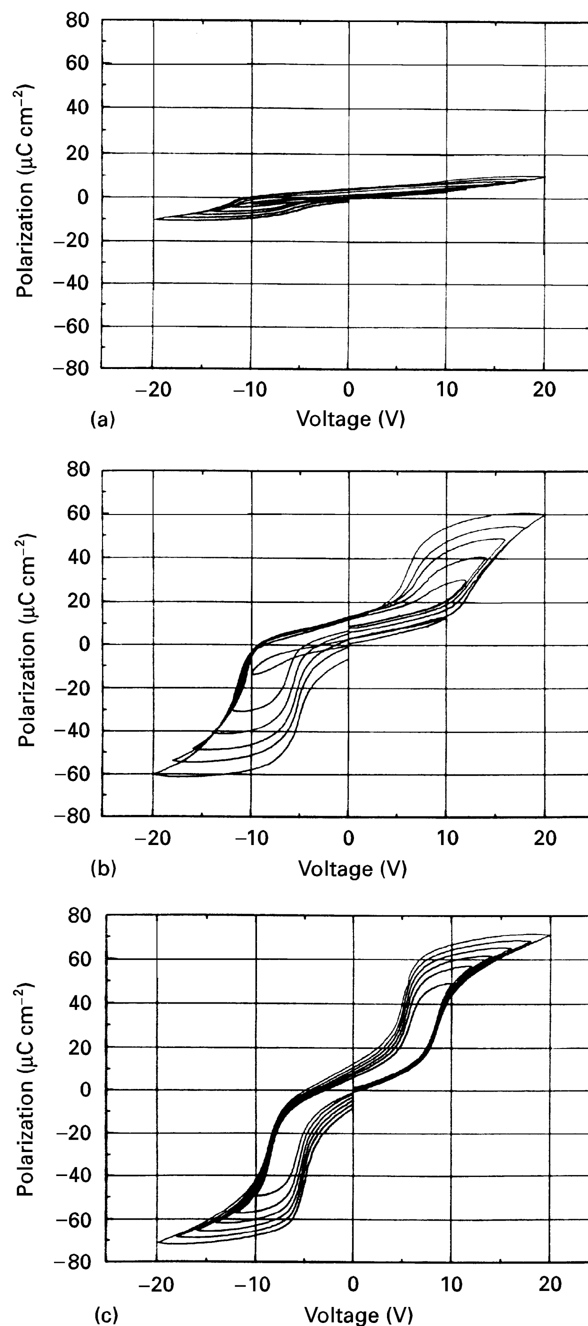

Figure 5 RTA temperature dependence of hysteresis loop; (a) 500 °C, (b) 600 °C, (c) 700 °C. Current for Pb was 49 mA.

Phase transformations at low temperature for $PbZrO_3$ films were also reported [22]. At 77 K, it was found that on increasing the field, an AFE–FE phase transformation similar to that seen at room

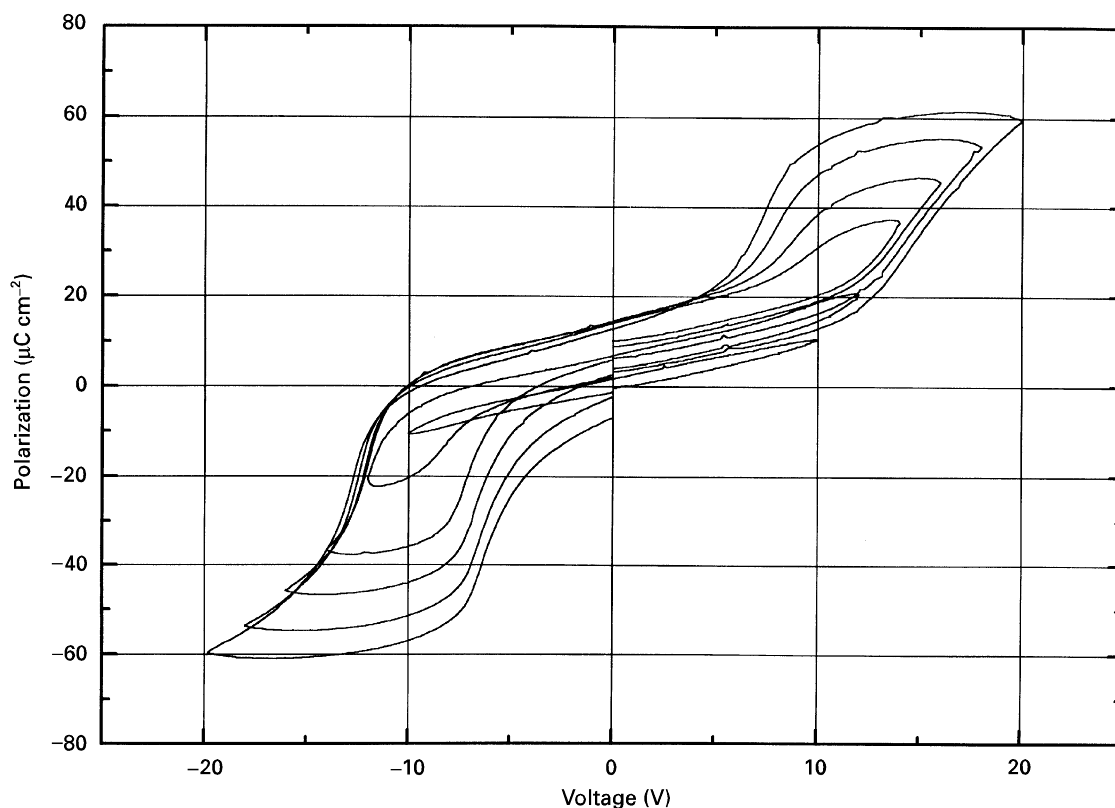

Figure 6 *D–V* hysteresis loop for 500 °C annealed film deposited at 52 mA. XRD pattern of this film is shown in Fig. 3.

temperature was observed. However, on decreasing the field, the FE phase converted to a metastable low-field FE phase (Fig. 7). That is, for virgin samples the AFE phase was obtained at low electric fields. Once exposed to a high field, however, a ferroelectric hysteresis loop was observed using modest fields. Fesenko *et al.* [6] found the same behaviour using $PbZrO_3$ single crystals. At temperatures lower than − 80 °C, once the orthorhombic FE phase of $PbZrO_3$ was induced by an electric field, it remained metastable after switching the field off, for an indefinitely long period. Moreover, a field of the reverse polarity did not return the crystal to its initial AFE state. Fig. 7 supports this result even in the case of thin films. The AFE–FE phase transformation can be obtained again by heating the samples above −80 °C as in [6].

3.3. Dielectric constant and I–V characteristics

The frequency dependence of the dielectric constant of films was measured using a MIM (metal-insulator-metal) configuration. The films exhibited a low field dielectric constant of about 160 and a dissipation factor of 0.05 at room temperature. The frequency dependent response indicated no dispersion below 1 MHz. There were a few differences observed in the dielectric constant and dissipation factor for the various Pb content films. The values of dielectric constant were between 150 and 180.

The temperature dependence of the dielectric constant is shown in Fig. 8. The measured sample was the 700 °C annealed film shown in Fig. 5. The data showed broad peaks of the dielectric constant for 1 kHz and 100 kHz measurement compared with that of bulk ceramics. The Curie temperature was 250 °C. It is believed that internal stress and defects in the films force the Curie temperature to be higher than that of 233 °C for ceramic $PbZrO_3$. This suggests that the internal stress and defects tend to favour the stabilization of the AFE phase. Because the AFE phase has a smaller molar volume than both the FE and paraelectric (PE) phases. The internal stress may be compressive in nature, as suggested earlier. However, one needs to confirm that the transitions with decreasing temperature are PE → AFE rather than PE → intermediate phase → AFE. The intermediate phase could be FE, AFE, etc.

The time dependence of leakage current is shown in Fig. 9. There was no polarity dependence observed. Conduction behaviour at higher electric fields was not obtained because of the instability of the films. This data was found to be consistent with that for PZT films reported before [23].

4. Conclusions

Antiferroelectric $PbZrO_3$ thin films with (240) preferred orientation on Pt coated Si substrates were prepared by a reactive magnetron co-sputtering method followed by a rapid thermal annealing process. The Pb content in the films affected the crystallization temperatures and the preferred orientations. It was found that the induced polarization values and electric fields of transformations changed with Pb content because of the presence of a PbO_x phase in

Figure 7 Field induced FE–FE phase transformation at 77 K. Electric field was increased on the left side and decreased on the right side.

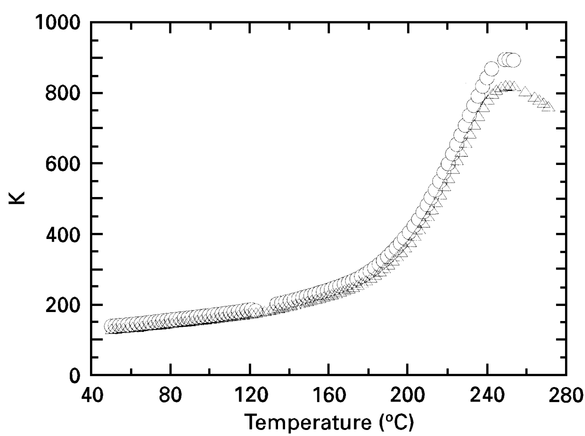

Figure 8 Temperature dependence of the dielectric constant; ○ 1 kHz, Δ 100 kHz.

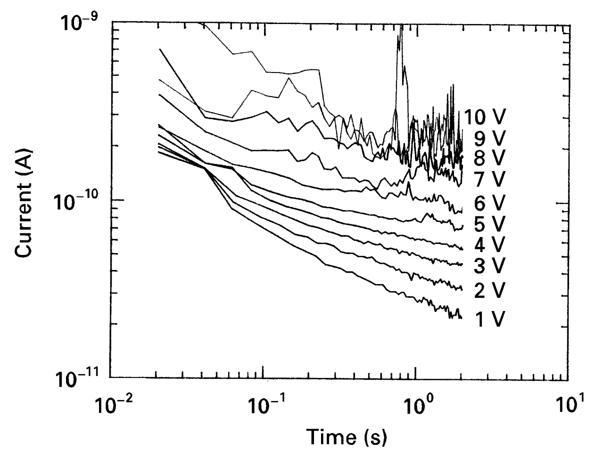

Figure 9 Time dependence of leakage current at various applied voltages.

Pb-rich films. The electric field forced transformation between the AFE–FE phases was observed at room temperature with a maximum polarization value of $70\,\mu C\,cm^{-2}$, an average field to excite the FE state of $290\,kV\,cm^{-1}$ and that for reversion to the AFE state of $180\,kV\,cm^{-1}$. An AFE–FE–FE irreversible transformation was also observed at 77 K. The room temperature, low field dielectric constant was around 160 with an associated loss of 0.07 at 1 MHz. The curie temperature was 248 °C at 1 kHz. The same type of conduction was observed in I–V measurement as that in PZT films.

References

1. M. SAYER, C. V. R. V. KUMAR, D. BARROW, L. ZOU and D. T. AMM, *Mater. Res. Soc. Symp. Proc.* **243** (1992) 39.
2. K. R. UDAYAKUMAR, "Ferroelectric Thin Films for Electronic Applications", Ph.D Thesis, The Pennsylvania State University, USA (1993).
3. J. M. HERBERT, "Ferroelectric Transducers and Sensors", Electrocomponent Science Monographs Vol. 3 (Gordon and Breach Science Publishers, 1982).
4. C. KITTEL, *Phys. Rev.* **82** (1951) 729.
5. G. SHIRANE, S. SAWAGUCHI and Y. TAKAGI, *ibid.* **84** (1951) 476.
6. O. E. FESENKO, R. V. KOLESOVA and YU. G. SINDEYEV, *Ferroelectrics* **20** (1978) 177.
7. W. Y. PAN, Q. M. ZHANG, A. BHALLA and L. E. CROSS, *J. Am. Ceram. Soc.* **72** (1989) 571.
8. K. G. BROOKS, J. CHEN, K.R. UDAYAKUMAR, *J. Appl. Phys.* **75** (1994) 1699.
9. R. P. BRODEUR, K. WA GACHIGI, P. M. PRUNA and T. R. SHROUT, *J. Am. Ceram. Soc.* **77** (1994) 3042.
10. K. D. BUDD, S. K. DEY and D. A. PAYNE, *Br. Ceram. Proc.* **36** (1985) 107.
11. F. WANG, K. K. LI and G. H. HAERTLING, *Opt. Lett.* **17** (1992) 1122.
12. G. R. BAI, H. L. M. CHANG, D. J. LAM and Y. GAO, *Appl. Phys. Lett.* **62** (1993) 1754.
13. T. TANI, J. F. LI, D. VIEHLAND and D. A. PAYNE, *J. Appl. Phys.* **75** (1994) 3017.
14. J. F. LI, D. D. VIEHLAND, T. TANI, C. D. E. LAKEMAN and D. A. PAYNE, *ibid.* **75** (1994) 442.
15. I. KANNO, S. HAYASHI, M. KITAGAWA, R. TAKAYAMA and T. HIRANO, *Appl. Phys. Lett.* **66** (1995) 145.
16. Y. AKIYAMA, S. KIMURA and I. FUJIMURA, *Jpn. J. Appl. Phys.* **32** (1993) 4154.
17. K. G. BROOKS, J. CHEN, K. R. UDAYAKUMAR and L. E. CROSS, *Mater. Res. Soc. Symp. Proc.* **243** (1992) 443.
18. C. J. GASKEY, "Electric Field Induced Antiferroelectric to Ferroelectric Phase Switching in Niobium Doped Lead Zirconate Stannate Titanate Thin Films," B. S. Thesis, The Pensylvania State University, USA (1993).
19. K. YAMAKAWA, S. TROLIER-McKINSTRY, J. P. DOUGHERTY and S. B. KRUPANIDHI, *Appl. Phys. Lett.* **67** (1995) 2014.
20. S. P. LEIPHART, "Reactive Co-sputtering Lead Titanate Thin Films," M. S. Thesis, The Pennsylvania State University, USA (1993).
21. K. YAMAKAWA, S. TROLIER-McKINSTRY and J. P. DOUGHERTY, submitted to *Thin Solid Films.*
22. K. YAMAKAWA, K. WA GACHIGI, S. TROLIER-McKINSTRY and J. P. DOUGHERTY, *Ferroelectr. Lett. Sect.* (in press).
23. H. HU and S. B. KRUPANIDHI, *J. Mater. Res.* **9** (1994) 1484.

Received 23 February 1996
and accepted 11 February 1997